JOURNAL OF GEOPHYSICAL RESEARCH, VOL. 98, NO. A3, PAGES 3501-3507, MARCH 1, 1993

Absolute Spectrum and Charge Ratio of Cosmic Ray Muons in the Energy Region From 0.2 GeV to 100 GeV at 600 m Above Sea Level

M. P. DE PASCALE,[1] A. MORSELLI,[1] P. PICOZZA,[1] R. L. GOLDEN,[2] C. GRIMANI,[2] B. L. KIMBELL,[2] S. A. STEPHENS,[2,3] S. J. STOCHAJ,[2] W. R. WEBBER,[2] G. BASINI,[4] F. BONGIORNO,[4,5] F. M. BRANCACCIO,[4] M. RICCI,[4] J. F. ORMES,[6] E. S. SEO,[6] R. E. STREITMATTER,[6] P. PAPINI,[7] P. SPILLANTINI,[7] M. T. BRUNETTI,[8] A. CODINO,[8] M. MENICHELLI,[8] AND I. SALVATORI[8]

We have determined the momentum spectrum and charge ratio of muons in the region from 250 MeV/c to 100 GeV/c using a superconducting magnetic spectrometer. The absolute differential spectrum of muons obtained in this experiment at 600 m above sea level is in good agreement with the previous measurements at sea level. The differential spectrum can be represented by a power law with a varying index, which is consistent with zero below 450 MeV/c and steepens to a value of -2.7 ± 0.1 between 20 and 100 GeV/c. The integral flux of muons measured in this experiment span a very large range of momentum and is in excellent agreement with the earlier results. The positive to negative muon ratio appears to be constant in the entire momentum range covered in this experiment within the errors and the mean value is 1.220 ± 0.044. The absolute momentum spectrum and the charge ratio measured in this experiment are also consistent with the theoretical expectations. This is the only experiment which covers a wide range of nearly 3 decades in momentum from a very low momentum.

1. INTRODUCTION

The energy spectrum and the charge ratio of muons at sea level have been studied extensively in the past over a wide range of energies. At high energies, the study of muons provides information on the composition of cosmic rays and interaction characteristics relevant to the propagation of cosmic rays in the atmosphere [e.g., *Badhwar et al.*, 1977]. At low energies, it is useful in estimating cosmogenic nuclei produced both in the atmosphere and in rocks [e.g., *Bilokon et al.*, 1989], neutrino induced events [e.g., *Gaisser et al.*, 1988] and in examining the effect of Earth's magnetic field on the propagation of secondary cosmic rays in the atmosphere [*Stephens*, 1979*a*]. The experimental study on muons was carried out above a few GeV using magnet spectrographs with electromagnets, in which charge particle trajectory is determined before and after traversing the magnetic field [e.g., *Ayre et al.*, 1973*a*]. In these spectrographs, charged particles pass through magnet blocks traversing large amounts of matter, and thus Coulomb scattering plays an important role in restricting the momentum resolution at low energies. Therefore at low energies, either low mass magnet spectrometers [*Allkofer and Dau*, 1972] or different techniques have been employed [*Singhal*, 1983, and references therein].

Most of the earlier measurements are limited to a small energy range. In order to interpret the spectral shape and charge ratio, which appear to vary with energy, it is essential that measurements be carried out at least over 2 decades in energy with a single instrument. Minimum amount of matter in the spectrometer is a necessity at low energies, where scattering plays an important role. An experiment which satisfied the above requirements was first carried out by *Stephens and Golden* [1987], using a superconducting magnet spectrometer. In the present experiment, we have used an improved design of the above instrument with an addition of an imaging calorimeter. This experiment covers a wide range in momentum from 0.25 GeV/c to 100 GeV/c. The data used here were gathered during a ground run on August 30, 1989, at Prince Albert, Saskatchewan, Canada. This location is at latitude 53°N and longitude 106°W, and is 600 m above sea level. Preliminary results from this experiment were reported earlier [*Basini et al.*, 1991] and in this paper we present the final results.

2. EXPERIMENTAL SETUP

Figure 1 shows the superconducting magnet spectrometer used for this experiment. This instrument was designed as a balloon-borne magnet spectrometer for cosmic ray studies [*Golden et al.*, 1991]. It consisted of the following detectors: (1) eight multiwire proportional chambers (MWPC) to record the particle trajectory, (2) a time of flight device (TOF) having two planes, each with two layers of scintillators ($T1$, $T2$) and ($T3$, $T4$) separated by a distance of 2.4 m to determine the direction and velocity, (3) TOF scintillators and an additional high-resolution scintillator $S1$ were used for the measurement of particle charge, (4) a gas Cherenkov counter filled with an equal mixture of freon 12 and freon 22

[1]Dipartimento di Fisica dell' Università di Roma "Tor Vergata," and INFN-Sezione di Roma II, Rome, Italy.
[2]Particle Astrophysics Laboratory, New Mexico State University, Las Cruces.
[3]Now at Tata Institute of Fundamental Research, Bombay, India.
[4]INFN-Laboratori Nazionali di Frascati, Rome, Italy.
[5]Now at Dipartimento di Metodi e Modelli Matematici dell' Università "La Sapienza," Rome, Italy.
[6]NASA Goddard Space Flight Center, Greenbelt, Maryland.
[7]Dipartimento di Fisica dell' Università di Firenze and INFN-Sezione di Firenze, Florence, Italy.
[8]Dipartimento di Fisica dell' Università di Perugia and INFN-Sezione di Perugia, Perugia, Italy.

Paper number 92JA02672.
0148-0227/93/92JA-02672$05.00

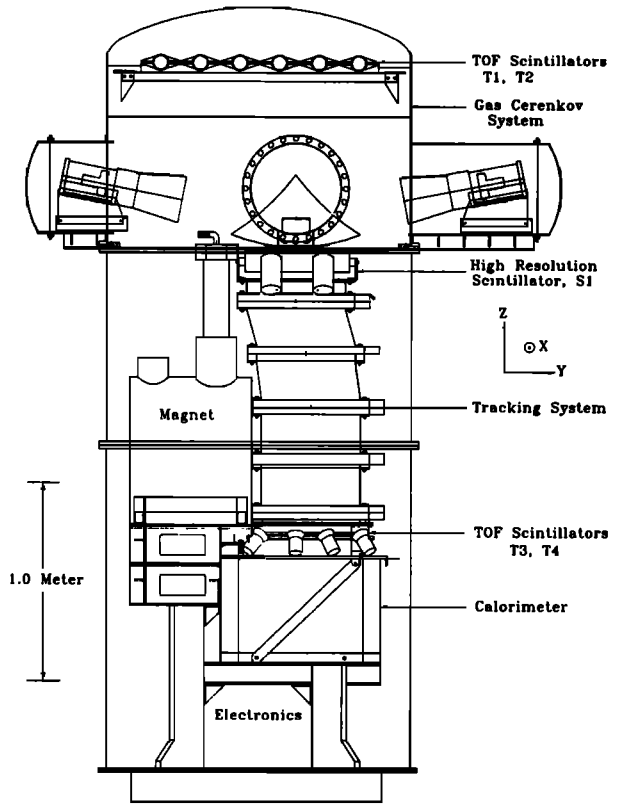

Fig. 1. A schematic diagram of the magnet spectrometer used in this experiment.

by volume, giving it a threshold Lorentz factor of 23, and (5) a calorimeter of size 50 cm × 50 cm × 40 cm (depth) and weight 418 kg was kept just below the scintillator $T4$. It consisted of 40 layers of 64 brass streamer tubes in which alternate layers were arranged perpendicular to each other. The walls of the streamer tubes served as the calorimeter material and the calorimeter had an effective depth of 7.33 radiation lengths, which is equivalent to 0.75 interaction mean free path for protons.

The superconducting magnet was operated at a current of 120 A, producing a magnetic field of 10 to 40 kG in the MWPC region. The maximum detectable magnetic rigidity (R = momentum/charge) was 118 GV/c. All MWPC were digitized in the X direction (the view which has the most curvature). Four MWPC were also digitized in the orthogonal view (Y direction). Delay line readout was used and the times of arrival at the MWPC were measured at each end of the delay lines [*Lacy and Lindsey*, 1974]. The sum of the delay line readout times was required to be equal to the total delay of the line in order for the data to be valid. Signals from all five scintillator layers and from the Cherenkov detector were pulse height analyzed. The calorimeter image data were gathered in digital form and algorithms can be applied directly to the data to perform nonsubjective tests. The performance of this detector is described in detail by *Golden et al.* [1991]. The trigger for an event was a coincidence between $T1$, $T2$, $T3$, and $T4$.

3. Data Analysis

3.1. *Selection of Events*

The criteria used for selecting muons for the analysis are summarized in Table 1. In this table, tests 1 to 4 are related to MWPC data. These tests were found to be very essential for a reliable determination of the particle curvature [*Golden et al.*, 1991]. It was found that the calorimeter was not 100% efficient in recording events in all the cells and at times spurious firing of some cells took place during the observation. Therefore tests 5 and 6 were introduced for selection of noninteracting particles passing through the calorimeter. For the purpose of selecting events, the calorimeter was divided into two nearly equal upper and lower parts, in order to make sure that the event passed through the entire calorimeter. Finally, test 7 was needed to select minimum ionizing singly charged particles. In this test, signals from $T1$ and $T2$ were chosen because the pulse height distributions from these scintillators were found to be narrow.

A total of 29,088 events passed the above tests and were selected for the analysis. These events were recorded over a period of 61,920 s. We have not used the signals from the Cherenkov detector for selecting a muon event. However, we have used the Cherenkov signal while examining individual events for the proton and electron contaminations in the sample and for determining the efficiency of the detectors.

3.2. *Geometrical Factor*

We have calculated the geometric factor (GF) for this instrument by requiring that the particle enter the instrument from $T1$ scintillator and leave by the bottom layer of the calorimeter. Further, the particle should traverse the sensitive area of all the detectors, except for the Cherenkov detector. We have shown in Figure 2 by a solid line, the calculated value of GF as a function of the deflection (d = 1.0/rigidity) of the particle. These calculations are accurate to 0.1%. It can be noticed that the GF decreases as the absolute value of the deflection increases. There is also a small difference between positively and negatively charged particles, especially at large values of absolute deflection. This difference is due to the mechanical asymmetry of the magnet with respect to the detector elements. For the negatively charged particles, the GF varies from 127.8 (cm^2

TABLE 1. Selection Criteria

Test	Description
1	a minimum of five X axis and three Y axis MWPC measurements should have good time sum
2	at least one of each pairs of the top, middle, and bottom X-MWPC, and the bottom Y-MWPC must be usable
3	the least squares fit to the reconstructed track must satisfy $\chi_x^2 \leq 5$ and $\chi_y^2 \leq 7.5$
4	the deflection uncertainty should be ≤ 0.03
5	at least N_{min} number of cells to be fired in each of the upper and lower parts of the calorimeter N_{min} = 3 in the X-Z plane N_{min} = 2 the Y-Z plane
6	there should not be more than N_{max} number of cells fired in X-Z plane N_{max} = 9 in the upper part N_{max} = 12 in the lower part
7	Signal S from $T1$ and $T2$ should be $0.5I_o \leq S \leq 2.0I_o$

sr) at rigidities $R > 5$ GV/c to 29.1 (cm^2 sr) at $R = 0.2$ GV/c, while for the positively charged particle it varies from 128.5 (cm^2 sr) for $R > 5$ GV/c to 27.6 (cm^2 sr) at $R = 0.2$ GV/c. It should be noted that one needs to correct for the particles, which satisfy tests 5 and 6 (Table 1), and escape through the side of the calorimeter, either by scattering or by magnetic deflection. One also needs to correct for the protons and a small fraction of electron events, which satisfy the above tests. These corrections will be discussed later.

3.3. *Efficiencies*

The detector efficiency relating to each set of tests described above was determined carefully. These are described below.

Spectrometer efficiency e_s: The overall efficiency of the spectrometer for particles satisfying tests 1 to 4 was found to be 0.69 ± 0.01 for $R > 4$ GV/c. This efficiency decreased with decreasing rigidity and was found to be dependent on the sign of the charge. We have determined this dependence by selecting events satisfying all criteria, other than tests 1 to 4, for a singly charged particle passing through the instrument. Visual examination of the calorimeter image was also made to remove electrons and protons from the sample of events, which satisfied the calorimeter cuts. This efficiency is shown in Figure 3 as a function of deflection. It can be noticed from this figure that the efficiency decreases very sharply below 1 GV/c. For the negatively charged particles this efficiency decreased to 0.433 ± 0.047 at $R = 0.22$ GV/c; for the positively charged particle it is 0.350 ± 0.038 at $R = 0.22$ GV/c. This asymmetry is due to the possible uncertainty in determining the exact position of the magnet center.

Calorimeter efficiency e_c: The efficiency of the calorimeter to detect a singly charged particle passing through it, was found to be 100% even though the individual cell efficiency was 82%. These efficiencies were determined by selecting a sample of high rigidity events satisfying all tests other than 5 and 6, and examining the response of streamer tubes along the trajectory of tracks. Due to the application of tests 5 and 6, some muons were lost. In order to estimate this inefficiency, events satisfying tests 1 to 4, 7 and the compliments of 5 and 6 were selected. This sample contains all the events lost due to the calorimeter cuts. These events were

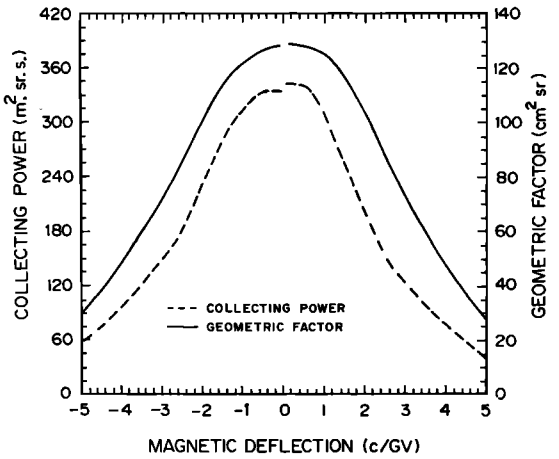

Fig. 2. The geometric factor and collecting power of the instrument are shown as function of the deflection of the particle.

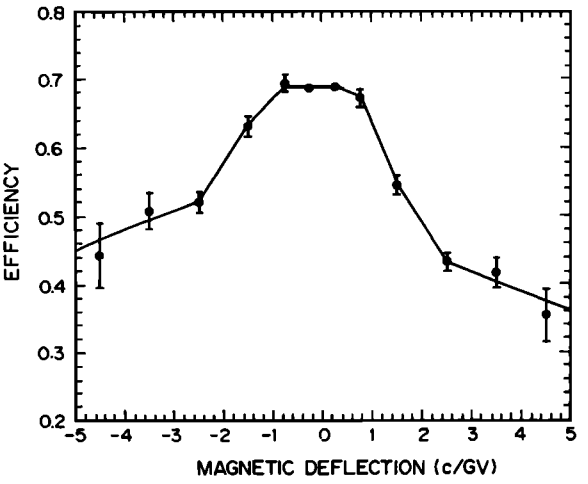

Fig. 3. The efficiency of the multiwire proportional chamber for events, which passed tests 1 to 4, is plotted as function of the deflection.

examined visually to identify muons using calorimeter image along with the reconstructed image through the spectrometer in both views [*Golden et al.*, 1991]. From this study the efficiency for recording muons passing tests 5 and 6 was determined and found to be 0.83 ± 0.01. This inefficiency results mainly due to the minimum number of hits required in each sector (test 5), because each calorimeter cell was only 82% efficient in recording events. The inefficiency arising from the restriction on the maximum number of hits (test 6) is due to the fact that at times spurious hits were registered outside the domain of the track, specially in the lower part of the calorimeter.

Scintillator efficiency e_s: The rejection of events due to the criteria used for the selection of singly charged particles by test 7 was estimated by examining the distribution of events in the high resolution scintillator $S1$. It was found that the efficiency by which particles satisfied test 7 is 0.91 with negligible error.

Other efficiency e_o: In addition to the above efficiencies, a tape reading efficiency of 0.93 was noticed. This inefficiency is due to the disk-write time of the ground computer being larger than the buffering capability of the input interface while transcripting the analog tapes. In addition to this, the dead time resulted in an efficiency of 0.98 for recording events. We also noticed an inefficiency in the trigger rate, because of the observed position dependent variation of the pulse height in $T1$, $T2$, $T3$, $T4$, and the fact that these scintillator planes were segmented. This was experimentally determined using small scintillator paddles for trigger and comparing the rates. It was estimated that the trigger efficiency in the experimental set up was 0.825. By combining these three efficiencies the value of e_o is 0.75 ± 0.01. There could be a possible systematic uncertainty of about 5%. The values of efficiencies are summarized in Table 2. One can notice from this table that 39% of the events above 2 GV/c survived the selection criteria, while at about 0.2 GV/c only 20% of the positive muons survived.

3.4. *Collecting Power*

In order to determine the collection power (CP) of the instrument for muons as a function of energy, one needs to

TABLE 2. Instrument Efficiencies in Selecting Events

Detector/ Function	Efficiency
Spectrometer	0.69 ± 0.01 above 2 GV/c dependent on energy and sign of charge below 2 GV/c (Figure 3)
Calorimeter	0.83 ± 0.01
Scintillators	0.91
Trigger	0.82 ± 0.01
Tape reading	0.93
Live time	0.98

determine the correction for scattering and magnetic deflection on the calculated GF as a result of the tests 5 and 6 (Table 1). It is also essential to estimate the effect of including a small fraction of e^- in the sample of negative muons and e^+ and protons in the sample of positive muons. Therefore a large sample of events which passed all the tests described earlier were chosen and the topology of each event in the calorimeter was examined visually. The above effects resulted in an overestimation of the negative muons by a factor of 1.159 ± 0.021 at R = 0.35 GV/c, which decreases to 1.087 ± 0.015 at $R > 2.5$ GV/c. In the case of positive muons, the corresponding factors are 1.159 ± 0.021 and 1.105 ± 0.016, respectively. It may be pointed out that protons that do not interact in the calorimeter are also taken into account in the above estimate. Let this correction be e_g. The CP is now defined as the product of GF, e_s, e_c, e_o, e_g, and the total time of observation.

We have shown in Figure 2 the estimated value of CP by the dashed curve as a function of deflection. The value of CP varies from 334.3 (m^2 sr s) for $R > 5$ GV/c to 49.3 (m^2 sr s) at R = 0.2 GV/c for negative muons. Similarly for the positive muons, the corresponding values are 342.0 (m^2 sr s) and 37.5 (m^2 sr s) respectively. We assume that all the errors associated with above efficiencies are independent of each other in evaluating the total error in the flux values for muons. As mentioned earlier, there could be possible systematic uncertainty of 5% in determining the absolute flux values. It may be emphasized that we have carried out a careful study of the energy dependence of the criteria for selecting the muon events.

4. RESULTS

The differential flux of muons is calculated after deconvolving the number spectrum of the observed muons using the spectrometer resolution function [*Golden et al.*, 1991] and by dividing the collecting power of the instrument. The observed differential flux per unit deflection is plotted as a function of deflection in Figure 4. The excess of positive muons can be seen specially at small deflections. In the same figure, we have shown the results from the previous experiment [*Stephens and Golden*, 1987] without the imaging calorimeter. One can notice that flux values in the previous experiment deviate from those of the present experiment for rigidities less than 3 GV/c. We believe that the underestimate of the flux values in the previous experiment at large deflection values is due to the inefficiencies associated with the selection criteria adopted in that analysis and the results below 3 GeV/c should be disregarded. Therefore we do not consider those results for later comparison with the present results.

4.1. *Differential Spectrum*

The absolute differential flux values of positive and negative muons are shown in Table 3 with errors. The median momentum in an interval has been calculated using the spectral shape. The values of momentum shown in this table are the muon momentum above the instrument, after being corrected for the ionization loss in the instrument. The number of muons shown in each momentum interval is the observed number before being deconvolved for the spectrometer resolution. The differential flux values of the total muons are plotted in Figure 5 and compared with those of *Allkofer et al.* [1971] and *Ayre et al.* [1973*a*] at sea level. The errors in data points in this figure are small compared to the size of the data points and one can notice a very good agreement with the earlier results. It can be noticed that the present spectrum has a very smooth spectral shape over more than 2 decades in momentum covering different experimental results. The spectrum is very flat at low energies having a spectral index consistent with zero below 0.45 GeV/c. This spectrum steepens gradually and the power law spectrum beyond 20 GeV/c has a spectral index of −2.7 ± 0.1. It may be pointed out that though the Allkofer et al. data overlap our results, those were obtained from experiments operating at three different energy bins using different spectrographs. The dashed curve in this figure above 1 GeV/c is the muon spectrum at sea level calculated by *Stephens* [1979*a*]. This calculation is based on the detailed formulation of this problem by *Badhwar et al.* [1977]. One can notice a general agreement between the calculated spectrum and the observed flux values over the entire energy region.

4.2. *Absolute Integral Spectrum*

The integral flux of muons was calculated by including muons above 100 GV/c. These flux values are shown in Table 4. One can notice that the errors at large momentum values are dominated by statistics, while at small momenta they are dominated by the errors in the estimated efficiencies. The absolute flux values 92.6 ± 2.3 muons/(m^2 sr s) at 0.321 GeV/c and 77.1 ± 1.8 at 0.722 GeV/c from this experiment are in good agreement with the values of 89.9 ±

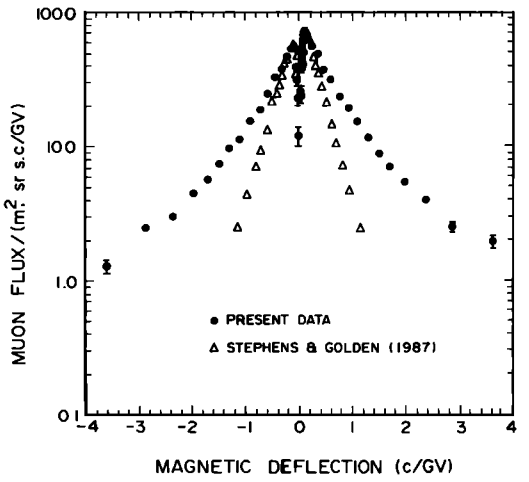

Fig. 4. Muon differential flux per unit deflection is plotted as a function of the deflection. The present results are compared with the data from an earlier experiment to show the possible inefficiency in the previous experiment at low energies.

TABLE 3. Differential Flux of Muons

Rigidity Interval, GV/c			Observed Number of Muons		Differential Flux (% Error) muons/(m^2 s sr GV/c)	
Minimum	Maximum	Median	Negative	Positive	Negative	Positive
0.247	0.321	0.283	133	164	0.1595E+2 (11.0)	0.2390E+2 (10.0)
0.321	0.393	0.356	231	188	0.2064E+2 (7.9)	0.2013E+2 (8.8)
0.393	0.463	0.428	232	260	0.1759E+2 (7.4)	0.2279E+2 (7.1)
0.463	0.564	0.513	418	439	0.1788E+2 (5.9)	0.2128E+2 (5.8)
0.564	0.633	0.598	299	326	0.1660E+2 (6.5)	0.2023E+2 (6.3)
0.633	0.722	0.677	418	442	0.1673E+2 (5.8)	0.1961E+2 (5.6)
0.722	0.841	0.780	577	637	0.1649E+2 (5.1)	0.1939E+2 (4.8)
0.841	1.008	0.922	698	904	0.1365E+2 (4.7)	0.1814E+2 (4.1)
1.008	1.198	1.101	795	794	0.1316E+2 (4.5)	0.1609E+2 (4.0)
1.198	1.478	1.334	992	1240	0.1094E+2 (4.1)	0.1328E+2 (3.6)
1.478	1.931	1.694	1313	1674	0.8756E+1 (3.7)	0.1093E+2 (3.2)
1.931	2.508	2.205	1299	1512	0.6789E+1 (3.6)	0.7705E+1 (3.3)
2.508	3.579	3.004	1514	1976	0.4244E+1 (3.3)	0.5404E+1 (2.9)
3.579	5.008	4.238	1252	1535	0.2634E+1 (3.5)	0.3145E+1 (3.1)
5.008	8.341	6.456	1408	1700	0.1274E+1 (3.3)	0.1506E+1 (3.1)
8.341	12.51	10.19	696	839	0.5025E+0 (4.3)	0.5983E+0 (3.9)
12.51	16.68	14.42	290	349	0.2124E+0 (6.2)	0.2523E+0 (5.7)
16.68	25.01	20.36	245	349	0.8653E−1 (6.7)	0.1246E+0 (5.7)
25.01	33.34	28.80	105	134	0.3788E−1 (9.9)	0.4709E−1 (8.8)
33.34	50.01	40.64	87	87	0.1389E−1 (11.5)	0.1430E−1 (11.3)
50.01	100.01	70.16	54	101	0.2423E−2 (15.8)	0.5176E−2 (10.7)

Read 0.1595E+2 as 0.1595 × 10^2.

0.05 at 0.353 GeV/c and 78.1 ± 0.5 at 0.725 GeV/c, respectively, of *Karmaker et al.* [1973]. Similarly, the present value of 86.9 ± 2.1 at 0.463 GeV/c is also in excellent agreement with the results of 87.5 ± 3.3 at 0.457 GeV/c by *Baschiera et al.* [1979]. However, the flux value determined by *Ashton et al.* [1972] at 0.88 GeV/c of 82.2 ± 4.0 differs from the present value of 72.9 ± 1.7 at 0.841 GeV/c. We have plotted in Figure 6 the absolute integral flux values from Table 4 along with the earlier measurements. It can be seen from this figure that there is excellent agreement between our results and those of others at energies below 1 GeV/c. The results of *Karmarkar et al.* [1979] deviate from our results above 1.5 GeV/c, and this could be due to not knowing the flux of muons above a few GeV/c accurately in their experiment. The dashed curve in this figure is the best fit line of *Allkofer et al.* [1971]; the error associated with this line is not given by the authors. This curve is also in excellent agreement with our results at least up to 10 GeV/c. This gives us confidence that our results are very reliable and that the quoted possible systematic uncertainty of 5% in determining the absolute flux is a conservative one. There is, however, some noticeable deviation above 50 GeV/c, which could partly be due to the momentum resolution in our experiment.

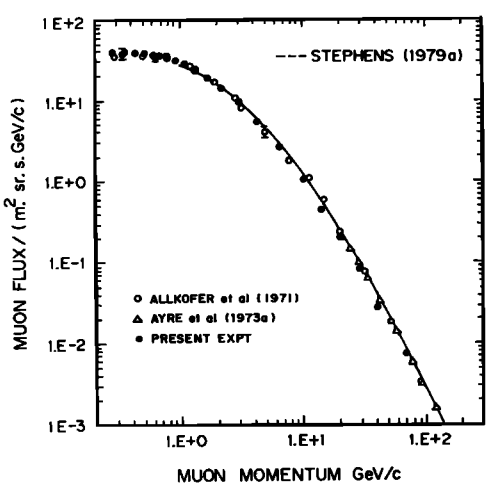

Fig. 5. The differential flux of the sum of the positive and negative muons is plotted as a function of momentum and is compared with earlier experiments with high statistics. The errors in this figure are smaller than the size of the data points. The dashed curve is a theoretical expectation.

TABLE 4. Integral Flux of Muons

Rigidity, GV/c	Integral Flux (% Error) muons/(m^2 sr s)		
	Negative Muons	Positive Muons	Total Muons
>0.247	0.4307E+2 (2.5)	0.5253E+2 (2.5)	0.9560E+2 (2.5)
>0.321	0.4189E+2 (2.5)	0.5075E+2 (2.5)	0.9264E+2 (2.5)
>0.393	0.4040E+2 (2.5)	0.4930E+2 (2.5)	0.8970E+2 (2.4)
>0.463	0.3917E+2 (2.4)	0.4771E+2 (2.4)	0.8689E+2 (2.4)
>0.564	0.3737E+2 (2.4)	0.4556E+2 (2.4)	0.8293E+2 (2.4)
>0.633	0.3622E+2 (2.4)	0.4416E+2 (2.4)	0.8037E+2 (2.3)
>0.722	0.3472E+2 (2.4)	0.4241E+2 (2.3)	0.7713E+2 (2.3)
>0.841	0.3276E+2 (2.4)	0.4010E+2 (2.3)	0.7286E+2 (2.3)
>1.008	0.3048E+2 (2.3)	0.3707E+2 (2.3)	0.6756E+2 (2.3)
>1.198	0.2798E+2 (2.3)	0.3401E+2 (2.3)	0.6199E+2 (2.2)
>1.478	0.2491E+2 (2.3)	0.3029E+2 (2.3)	0.5520E+2 (2.2)
>1.931	0.2095E+2 (2.3)	0.2534E+2 (2.3)	0.4630E+2 (2.2)
>2.508	0.1703E+2 (2.4)	0.2090E+2 (2.3)	0.3793E+2 (2.2)
>3.579	0.1249E+2 (2.5)	0.1511E+2 (2.4)	0.2760E+2 (2.3)
>5.008	0.8724E+1 (2.7)	0.1062E+2 (2.6)	0.1934E+2 (2.4)
>8.341	0.4478E+1 (3.3)	0.5596E+1 (3.1)	0.1008E+1 (2.6)
>12.51	0.2384E+1 (4.1)	0.3103E+1 (3.7)	0.5487E+1 (3.1)
>16.68	0.1499E+1 (4.9)	0.2052E+1 (4.3)	0.3551E+1 (3.5)
>25.01	0.7779E+0 (6.5)	0.1014E+1 (5.7)	0.1792E+1 (4.5)
>33.34	0.4623E+0 (8.3)	0.6214E+0 (7.2)	0.1084E+1 (5.6)
>50.01	0.2308E+0 (12.0)	0.3831E+0 (9.0)	0.6139E+0 (8.0)
>100.01	0.1096E+0 (17.0)	0.1243E+0 (16.0)	0.2339E+0 (15.0)

Read 0.4307E+2 as 0.4307 × 10^2.

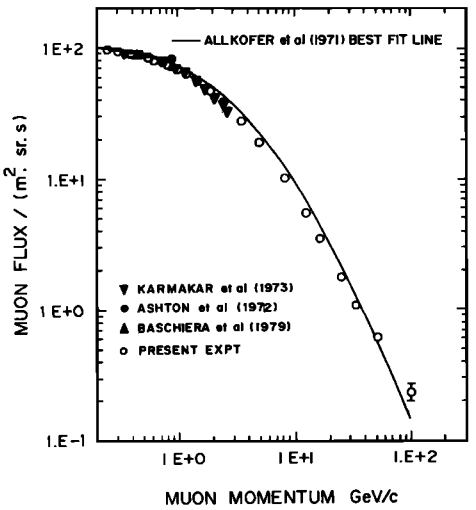

Fig. 6. The integral rate is plotted as a function of momentum and compared with the earlier data. The dashed curve is the best fit to observed data of *Allkofer et al.* [1971].

4.3. *Charge Ratio*

The charge ratios for the muons were estimated by combining different flux bins and are shown in Table 5. It can be noticed that the charge ratio remains nearly the same within errors over the entire energy region. The mean value of charge ratio between 0.247 and 100 GeV/c is found to be 1.220 ± 0.044. These results are plotted as a function of momentum in Figure 7 along with a few other results. The solid curve shown in this figure is the expected ratio [*Stephens*, 1979*b*]. It is very clear from this plot that no experiment which measured the ratio above a few GeV/c was able to extend the measurement to lower momenta. Thus the present experiment is unique in determining the charge ratio over a wide momentum region in a reliable manner. It can be noticed that at momenta greater than a few GeV/c, the existing results [e.g., *Rastin*, 1984; *Ayre et al.*, 1973*b*] have small errors, and the charge ratio is rather well defined. The present results in this domain are in agreement

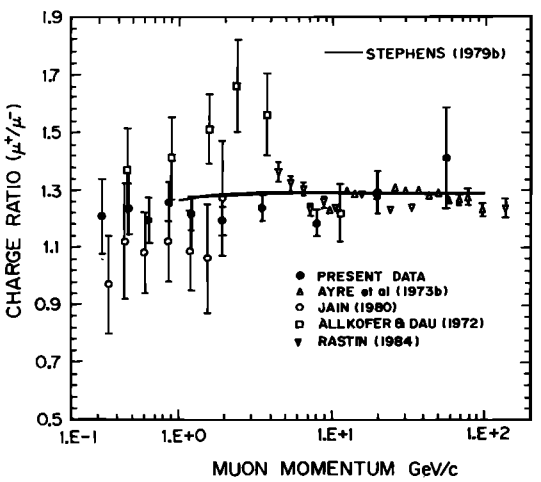

Fig. 7. Positive to negative charge ratio of muons is plotted as a function of momentum along with some other existing data. The solid curve is a theoretical prediction by *Stephens* [1979*b*].

TABLE 5. Observed Charge Ratio of Muons

Rigidity Interval, GV/c			
Minimum	Maximum	Median	Charge Ratio
0.247	0.393	0.320	1.207 ± 0.130
0.393	0.564	0.479	1.233 ± 0.088
0.564	0.722	0.643	1.192 ± 0.081
0.722	1.008	0.865	1.258 ± 0.068
1.008	1.478	1.228	1.218 ± 0.057
1.478	2.508	1.948	1.192 ± 0.049
2.508	5.008	3.568	1.237 ± 0.046
5.008	12.51	8.008	1.185 ± 0.047
12.51	33.34	19.89	1.292 ± 0.075
33.34	100.01	55.87	1.409 ± 0.173

with these data. These data are also very consistent with the expected ratio [e.g., *Badhwar et al.*, 1977; *Stephens*, 1979*b*]. However, the results obtained so far on the charge ratio below a few GeV/c have very large errors and disagree among themselves [*Jain*, 1980; *Allokofer and Dau*, 1972]. The results obtained in the present experiment have smaller errors compared to other experiments and are consistent with the extension of the theoretical expectations. It is essential to improve the statistical significance of the results in the entire energy domain considered here by long exposure experiments, in order to draw meaningful conclusions.

Acknowledgments. This work was supported by NASA grant NAG-110, the Istituto Nazionale di Fisica Nucleare, Italy, and the Agenzia Spaziale Italiana. We wish to record our special thanks to our technical support staff from NMSU and INFN.

The Editor thanks M. Shapiro and another referee for their assistance in evaluating this paper.

REFERENCES

Allkofer, O. C., and W. D. Dau, The muon charge ratio at sea level in the low momentum region, *Phys. Lett.*, *38B*, 439–440, 1972.

Allkofer, O. C., K. Carstensen, and W. D. Dau, The absolute cosmic ray muon spectrum at sea level, *Phys. Lett.*, *36B*, 425–428, 1971.

Ashton, F., K. Tsuji, and A. W. Wolfendale, The absolute vertical cosmic ray muon intensity at sea level, *Nuovo Cimento*, *9B*, 344–350, 1972.

Ayre, C. A., J. M. Baxendale, B. J. Daniel, C. J. Hume, M. G. Thompson, M. R. Whalley, and A. W. Wolfendale, The absolute muon spectrum in the range 3.5–700 GeV/c in the near vertical direction, *Conf. Pap. Int. Cosmic Ray Conf. 13th*, *3*, 1754–1763, 1973*a*.

Ayre, C. A., J. M. Baxendale, B. J. Daniel, C. J. Hume, B. C. Nandi, M. G. Thompson, M. R. Whalley, and A. W. Wolfendale, The muon charge ratio in the near vertical direction the range 10–450 GeV/c, near vertical direction, *Conf. Pap. Int. Cosmic Ray Conf. 13th*, *3*, 1822–1827, 1973*b*.

Badhwar, G. D., S. A. Stephens, and R. L. Golden, Analytic representation of the proton-proton and proton-nuclus cross-sections and its application to the sea-level spectrum and charge ratio of muons, *Phys. Rev.*, *D15*, 820–831, 1977.

Baschiera, B., G. Basini, H. Bilokon, B. D'Ettorre Piazzoli, G. Mannocchi, C. Castagnoli, and P. Picchi, Integral and differential absolute intensity measurements of muons below 1 GeV, *Nuovo Cimento Soc. Ital. Fis. C*, *2*, 473–486, 1979.

Basini, G., et al., Cosmic ray muon spectrum and charge ratio between 0.2 and 100 GeV at 600 meters above sea level, *Conf. Pap. Int. Cosmic Ray Conf. 22nd*, *4*, 544–547, 1991.

Bilokon, H., G. C. Castagnoli, A. Castellina, B. D'Ettorre Piazzoli, G. Mannocchi, E. Meroni, P. Picchi, and S. Vernetto, Flux of vertical negative muons stopping at depths 0.35–1000 hg/cm^2, *J. Geophys. Res.*, *94*(B9), 12,145–12,152, 1989.

Gaisser, T. K., T. Stanev, and G. Barr, Cosmic ray neutrinos in the atmosphere, *Phys. Rev., 38D*, 85–95, 1988.

Golden, R. L., et al., Performance of a balloon-borne magnet spectrometer for cosmic ray studies, *Nucl. Instrum. Meth., A306*, 366–377, 1991.

Jain, S. K., Vertical cosmic ray muon flux and charge ratio in the momentum region (0.3 GeV/c–2 GeV/c), *Proc. Indian Natl. Sci. Acad., Sect. A, 46*, 149–157, 1980.

Karmakar, N. L., K. Paul, and N. Chaudhuri, Measurements of absolute intensities of cosmic ray muons in the vertical and greatly inclined directions at geomagnetic latitudes 16°N, *Nuovo Cimento, 17B*, 173–186, 1973.

Lacy, J. L., and R. S. Lindsey, High resolution readout of multiwire proportional counters using the cathode coupled delay-line technique, *Nucl. Instrum. Meth., 119*, 83–498, 1974.

Rastin, B. C., A study of the muon charge ratio at sea level within the momentum range 4 to 2000 GeV/c, *J. Phys. G Nucl. Part. Phys., 10*, 1629–1638, 1984.

Singal, K. P., Determination of charge ratio of low energy cosmic ray muons, *Conf. Pap. Int. Cosmic Ray Conf. 18th, 7*, 27–30, 1983.

Stephens, S. A., An examination of zenith angle dependence of spectrum at sea-level, *Conf. Pap. Int. Cosmic Ray Conf. 16th, 10*, 90–95, 1979*a*.

Stephens, S. A., Charge ratio of muons at sea-level and its dependence on zenith angle, *Conf. Pap. Int. Cosmic Ray Conf. 16th, 10*, 96–101, 1979*b*.

Stephens, S. A., and R. L. Golden, Determination of the energy spectrum and charge composition of muons at sea-level, *Conf. Pap. Int. Cosmic Ray Conf. 20th, 6*, 173–176, 1987.

G. Basini, F. M. Brancaccio, and M. Ricci, INFN–Laboratori Nazionali di Frascati, Via Enrico Fermi, 40, 00044 Frascati, Roma, Italy.

F. Bongiorno, Dipartmento di Metodi e Modelli Matematici dell' Università "La Sapienza," Piazzale A. Moro 2, 00185 Roma, Italy.

M. T. Brunetti, A. Codino, M. Menichelli, and I. Salvatori, Departimento di Fisica dell' Università di Perugia and INFN–Sezione di Firenze, Largo Enrico Fermi, 2, 50125 Firenze, Italy.

M. P. De Pascale, A. Morselli, and P. Picozza, Dipartimento di Fisica dell' Università di Roma "Tor Vergata," and INFN–Sezione di Roma II, Via Emanuele Carnevale, 15, 00173 Roma, Italy.

R. L. Golden, C. Grimani, B. L. Kimbell, S. J. Stochaj, and W. R. Webber, Particle Astrophysics Laboratory, New Mexico State University, Las Cruces, NM 88003.

J. F. Ormes, E. S. Seo, and R. E. Streitmatter, NASA Goddard Space Flight Center, Greenbelt, MD 20771.

P. Papini and P. Spillantini, Dipartimento di Fisica dell' Università di Firenze and INFN–Sezione di Firenze, Largo Enrico Fermi, 2, 50125 Firenze, Italy.

S. A. Stephens, Tata Institute of Fundamental Research, Homi Bhabha Road, Bombay 400 005, India.

(Received July 15, 1992;
revised October 7, 1992;
accepted October 14, 1992.)